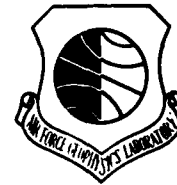


LEVEL II

12

AFGL-TR-80-0277
INSTRUMENTATION PAPERS, NO. 291



57

**The Problem: Instantaneously
Effecting Controlled Balloon-System
Descent From High Altitude**

JAMES F. DWYER



11 September 1980

Approved for public release; distribution unlimited.

DTIC FILE COPY

AEROSPACE INSTRUMENTATION DIVISION PROJECT 7659
AIR FORCE GEOPHYSICS LABORATORY
HANSCOM AFB, MASSACHUSETTS 01731

AIR FORCE SYSTEMS COMMAND, USAF



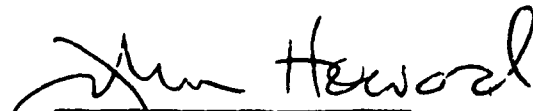
81 6 15 137

+

This report has been reviewed by the ESD Information Office (OI) and is releasable to the National Technical Information Service (NTIS).

This technical report has been reviewed and is approved for publication.

FOR THE COMMANDER



Chief Scientist

Qualified requestors may obtain additional copies from the Defense Technical Information Center. All others should apply to the National Technical Information Service.

Unclassified

SECURITY CLASSIFICATION OF THIS PAGE (When Data Entered)

REPORT DOCUMENTATION PAGE		READ INSTRUCTIONS BEFORE COMPLETING FORM
1. REPORT NUMBER AFGL-TR-80-0277	2. GOVT ACCESSION NO. AD-A100 255	3. REPORT/CATALOG NUMBER
4. TITLE (and Subtitle) THE PROBLEM: INSTANTANEOUSLY EFFECT- ING CONTROLLED BALLOON-SYSTEM DESCENT FROM HIGH ALTITUDE	5. TYPE OF REPORT/PERIOD COVERED Scientific, Final.	6. PERFORMING ORG. REPORT NUMBER IP No. 291
	7. AUTHOR(S) James F./Dwyer	8. CONTRACT OR GRANT NUMBER
9. PERFORMING ORGANIZATION NAME AND ADDRESS Air Force Geophysics Laboratory (LCA) Hanscom AFB Massachusetts 01731	10. PROGRAM ELEMENT PROJECT TASK AREA & WORK UNIT NUMBERS 62101F 76591102	12. REPORT DATE 11 September 1980
11. CONTROLLING OFFICE NAME AND ADDRESS Air Force Geophysics Laboratory (LCA) Hanscom AFB Massachusetts 01731	13. NUMBER OF PAGES 38	15. SECURITY CLASS. of this report Unclassified
14. MONITORING AGENCY NAME & ADDRESS (if different from Controlling Office)	16. DISTRIBUTION STATEMENT (of this Report) Approved for public release; distribution unlimited.	15a. SECURITY CLASSIFICATION DOWNGRADING SCHEDULE
17. DISTRIBUTION STATEMENT (of the abstract entered in Block 20, if different from Report)	18. SUPPLEMENTARY NOTES	
19. KEY WORDS (Continue on reverse side if necessary and identify by block number) Free balloons Float stability Descent control Vertical motion Shape models Valve efficiency	20. ABSTRACT (Continue on reverse side if necessary and identify by block number) The need for a technique to instantaneously effect controlled balloon- system descent from high altitude prompted the development efforts reported herein. The background, the approach, test flight data, and the technical problems that frustrated the successful development of the desired technique are included. A simplified model of the shape of a partially full balloon is presented (a model that should also approximate the dimensions of subpressure shapes). Some heretofore unpublished information on apex valve characteris- tics and subpressure effects are included together with recommendations for	

Unclassified

SECURITY CLASSIFICATION OF THIS PAGE (When Data Entered)

Unclassified

SECURITY CLASSIFICATION OF THIS PAGE (When Data Entered)

20. Abstract (Continued)

any future work of this problem. Significant supplementary findings and historical perspectives are noted.

Unclassified

SECURITY CLASSIFICATION OF THIS PAGE (When Data Entered)

Contents

1. INTRODUCTION	7
2. BACKGROUND	7
3. ORIGIN OF THE PROBLEM	10
4. THE SIMPLE APPROACH	11
5. THE SOPHISTICATED APPROACH	16
6. CONCLUSIONS	24
7. THE NEXT STEPS	25
8. SUPPLEMENTARY RESULTS	26
REFERENCES	29
APPENDIX A: Notes on Flight C72-21	31
APPENDIX B: The Simplified Parachute-Shape Model	33

Illustrations

1. Conventional Modern Plastic Balloon Components Consist of: 1) inflation or fill tube, 2) apex fitting, 3) strobe light, 4) electric valve, 5) destruct button at apex of rip panel "V" tapes (two of these are usual and they are activated by a line which passes from the payload-parachute up through the balloon and is secured to them), 6) gore panel (usually about 100 inches wide), 7) load tapes, 8) pressure relief duct, and 9) base end fitting with load ring for payload suspension	8
2. Apex Valve Efficiency	10
3. Schematic of Balloon Features Related to the Exhaust Duct Function	13
4. Pictorial Representation of the Flexibility Provided by Construction of the Exhaust Duct as a Conventional Ascent Valving Duct	14
5. Volume Expressed as a Fraction of Maximum Balloon Volume in Relation to the Nondimensionalized Gore Length Distance, S_D , from the Nadir to the Exhaust Duct Outlet or Zero Pressure Differential Level	15
6. Simplified Parachute Shape Model	17
A1. Historical Trends	32
B1. Essential Features of the Simplified Parachute Shape Model	34
B2. Plot of Data Points Used in the Functions that Model \bar{z} in Terms of V_2/V_{\max}	36

Tables

1. Balloon Performance With a Drag Coefficient of 0.5	19
2. Balloon Performance With a Drag Coefficient of 1.0	20
3. Characteristics of Flight Test Balloon, AFGI Model No. LTV-026, Equipped With Stub Exhaust Ducts	21
4. Time-Altitude System Response of Flight H79-32	21
5. Time-Altitude System Response of Flight H79-34	22
B1. Functions Comprising Model to Solve for \bar{z} as a Function of V_2/V_{\max}	37
B2. Power Series Coefficients for Equations Defining Certain Relationships Between Elements of the Simplified Parachute Shape Model	38

The Problem: Instantaneously Effecting Controlled Balloon-System Descent From High Altitude

1. INTRODUCTION

The capability¹ of the present-day, helium-filled, plastic balloon far exceeds that demonstrated by the first balloon launched publicly by the Montgolfier brothers at Annonay, France, in 1783. Full realization of today's potential capability, however, depends on further technological advances that will be equally as complex and important as those that established the present state-of-the-art. Two areas wherein significant advancements are required are ascent control and descent control. One special example of the latter is the subject of this paper: the development of a method for achieving a quick response, controlled descent from high altitudes.

2. BACKGROUND

Scientific ballooning utilizing large plastic balloons (see Figure 1) had its beginnings in the 1940s. In those days, changes in ascent and descent rates were effected by either timer or pressure-activated ballast drops; those methods were

(Received for publication 11 September 1980)

1. Dwyer, J. E. (1974) Free balloon capabilities: a critical perspective, in Proceedings (Supplement), Eight AFCL Scientific Balloon Symposium, 30 September to 3 October 1974, AFCL-TR-74-0596, AD A003 489, pp 123-156.

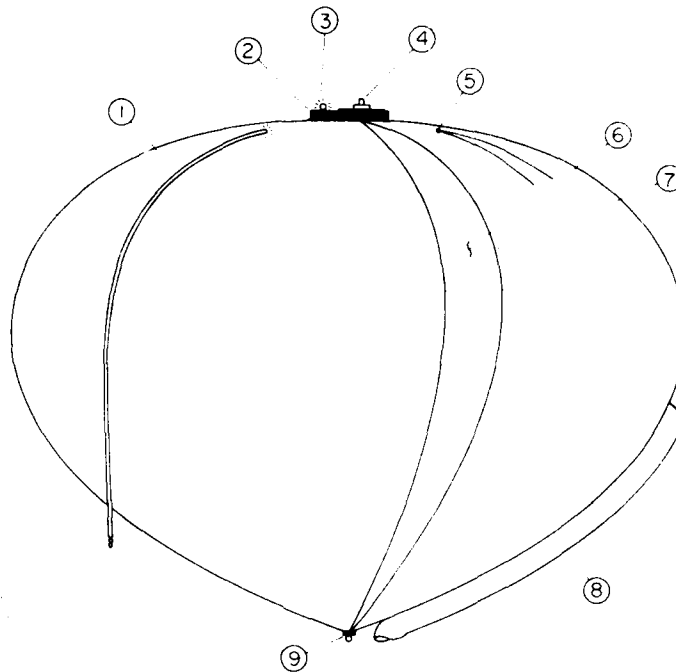


Figure 1. Conventional Modern Plastic Balloon Components
 Consist of: 1) inflation or fill tube, 2) apex fitting,
 3) strobe light, 4) electric valve, 5) destruct button at
 apex of rip panel "V" tapes (two of these are usual and they
 are activated by a line which passes from the payload-para-
 chute up through the balloon and is secured to them),
 6) gore panel (usually about 100 inches wide), 7) load
 tapes, 8) pressure relief duct, and 9) base end fitting with
 load ring for payload suspension

adequate then because mission objectives did not require complex flight profiles, dependent on sophisticated vertical control techniques. With respect to terminal descent, neither the altitudes attainable nor the payload capacities presented a formidable problem for the conventional recovery parachute.

Vertical control dating to the very early aerostats was routinely continued in the manned scientific balloon flights² of the 1950s. Control was accomplished by the use of ballast and a valve located in the apex of the balloon. However, where the early aeronauts relied on a rope to open and close the valve, modern valves are operated electrically.

2. Schwoebel, R. L. (1956) Strato-lab Development, General Mills, Inc., Report No. 1648, Final Report, Contract No. NONR 1589(06).

For the most part, on early unmanned flights into the stratosphere, the payloads were equipped with a recovery parachute flown in a packed configuration. Transfer of the payload from the balloon to the recovery parachute was effected by a small drogue parachute which extracted the packed parachute when line cutters severed the line between the balloon and the payload. The use of the packed parachute was discontinued in the mid 1950's, partially as a result of the introduction of multiple-package payloads and partially to ensure parachute opening and payload recovery in the event of balloon burst. Packed parachute recovery systems were replaced with parachutes flown fully extended and loaded, in-line between the balloon and the payload. Parachutes flown in this configuration respond to the sudden and rapid system descent, at balloon burst, by partially blossoming. This blossoming action provides the means of activating a circuit* to open the load link between the balloon base and parachute apex.

Interactive control, always desirable, became practical with the development of reliable airborne telemetry and command systems, but problems still remained. With the passage of time required for these developments, both altitude and payload requirements had grown. Increased altitudes, of course, reduce the efficiency of the apex valve, whereas increased payload and altitude combine to place added demands on the recovery parachute system.

The adverse impact on apex valve effectiveness follows from the dependence of flow rate on valving pressure differential and from the variation in the valve discharge coefficient with reduced pressure differential. The flow rate has been shown to be proportional to the $2/3$ power of the specific lift of the inflatant,³ which diminishes almost exponentially with altitude; the valve discharge coefficient is shown graphically in Figure 2.

Increased requirements produced two recovery parachute problems: opening shock and parachute stability. With the reduced density at very high altitudes, a greater descent velocity is required to achieve the dynamic pressure to inflate the parachute, and this higher descent velocity generates a greater opening shock. The instability of the free-falling system at very high altitudes prior to full parachute deployment may result in tumbling and free fall with resultant payload loss. In this regard, upward looking cameras[†] on balloon flight number C72-21 from Chico, California, on 26 October 1972 clearly revealed that the falling payload

* In the literature, the mechanism that performs this function is generally found under the title "burst switch."

3. Dwyer, J. F. (1973) Balloon Apex Pressure Differential, AFCRL-TR-73-0632, AD 774 399.

† These cameras also revealed that the standard reefing sleeve, designed to control the deployment of balloon film, hung up. This fostered the development of a discontinuous reefing sleeve now used on a majority of large Air Force balloons.

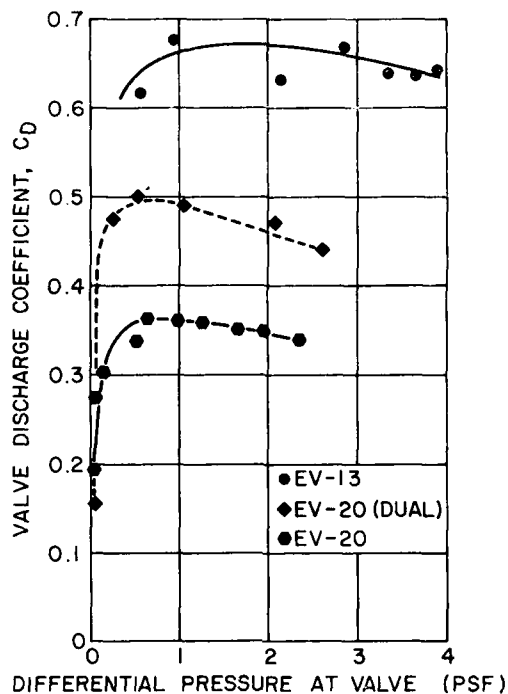


Figure 2. Apex Valve Efficiency. The importance of these data, obtained from unpublished flow rate tests, lies in their trend toward reduced efficiency at the lower differential pressures. The significance of this becomes clear when one considers that a 4000 pound system at 120,000 feet would have a differential pressure of only 0.074 pounds per square foot

system was inverted during part of the recovery parachute deployment sequence. This happened when a 370-lb payload was released on a flat circular parachute, 40 ft in diameter, from a balloon, 47.8 million cu ft in volume floating at a record altitude of about 170,000 ft (see also Appendix A).

3. ORIGIN OF THE PROBLEM

An early system requirement emphasized the need for developing solutions to descent-control problems. Specifically, a sensitive telescope system floating in the vicinity of 100,000 ft at sunrise had to be lowered quickly, but gently, to about 50,000 ft. This altitude change was essential for two reasons: (1) optimum landing area selection required the ability to rapidly change float altitude to take

advantage of more favorable wind fields, and (2) the reduced parachute opening shock achievable at the lower altitude would minimize the time and effort needed to refurbish and reflly the system.

Methods of effecting controlled descent were resolved into two exclusive categories: those in which the initiating sub-system could be returned to its original state, and those in which it could not. For example, an electric motor-driven apex valve, as is the conventional model EV-13, is typically in the former category. On the other hand, a squib activated frangible plate of comparable size installed in the apex fitting would produce the same initial effect when activated under identical conditions, but it could not be returned to its initial state. The reaction in the latter case would likewise not be reversible (a requirement for other than simple up-down flight profiles).

4. THE SIMPLE APPROACH

For three reasons the following described approach was selected for the first attempt at effective, quick response, controlled descent. First, it potentially solved the immediate problems of quickly reducing the parachute deployment altitude and of rapidly attaining a lower floating altitude compatible with safe impact and recovery. Second, the method could accommodate the simple up-down flight profiles which are the most common profiles due to flight time limits imposed by acceptable horizontal displacement. Finally, the selected approach was economically sound (based on proven balloon design and manufacturing practices) and it would not jeopardize the primary mission of the balloon flights by which it was to be evaluated.

Given a suitably located and reasonably sized hole, the venting of a determinable volume of inflatant was never considered to be a problem. On the contrary, even small holes located relatively low in the balloon were considered significantly detrimental to relatively short duration flights.* Establishment of criteria for the location and size of a suitably configured exhaust duct was thus considered to be the principal component of the selected simple approach.

The lower portion of a conventional free balloon floating at its natural ceiling altitude has, for practical purposes, a conical shape. It was reasoned that a cylindrical duct located in the wall of this conical section would, when opened to the atmosphere, quickly exhaust a volume of inflatant not greater than that of the conical volume below it. The flow rate was expected to be comparable to that of a valve of equivalent size and location, and the time required to exhaust the cone

*The flight of one balloon designed to utilize the selected approach, discussed in the conclusions, provides some interesting information to the contrary.

was expected to be short enough to preclude appreciable balloon system descent. It was recognized, however, that any flow would cause reduction of the pressure within the conical volume and would thus limit flow rate, a further safeguard against valving too much inflatant.

Assuming the geometrical configuration of Figure 3 and non-viscous, incompressible gas flow, V (the volume of inflatant above the plane of the zero pressure level) and u (the duct discharge velocity in feet per second) can be written as

$$V = \pi \tan^2 \theta (X_0^2 X - X_0 X^2 + X^3/3) \quad (1)$$

$$u = \sqrt{2gX} \quad , \quad (2)$$

so that the corresponding volumetric change and flow rate become:

$$dV = \pi \tan^2 \theta (X - X_0)^2 dX \quad (3)$$

$$dV = -C_D A_D \sqrt{2gX} dt \quad , \quad (4)$$

where:

C_D is the dimensionless duct discharge coefficient.

A_D is the duct cross-sectional area in square feet.

These two relationships yield T (the time in seconds) as:

$$T = \int_0^t dt = \frac{\pi \tan^2 \theta}{C_D A_D \sqrt{2g}} \int_0^{X_0} \left[(X - X_0)^2 / \sqrt{X} \right] dX \quad (5)$$

$$T = \frac{16 \pi \tan^2 \theta}{15 C_D A_D \sqrt{2g}} \sqrt{X_0^5} \quad . \quad (6)$$

Where the conically approximated volume is determined by:

$$V_C = \pi \tan^2 \theta X_0^3 / 3 \quad , \quad (7)$$

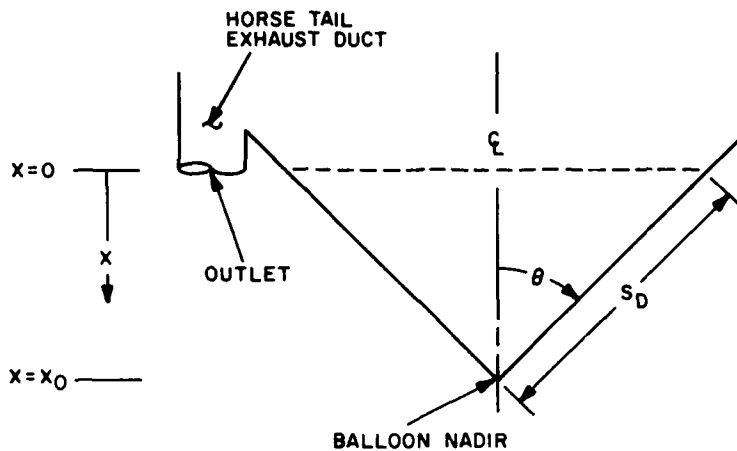


Figure 3. Schematic of Balloon Features Related to the Exhaust Duct Function

T and S_D (the lower extremity of the exhaust duct, measured in feet upward along the gore from the base fitting) become:

$$T = \frac{0.402 \tan^{1.3} \theta}{C_D A_D} V_C^{5.6} \quad (8)$$

and

$$S_D = [3V_C / (\pi \cos \theta \sin^2 \theta)]^{1/3} \quad (9)$$

Now, given the problem of establishing a specified negative lift at a specified altitude, Eq. (9) could be used to establish the location of the duct's lower extremity (outlet), and Eq. (8) to yield the minimum exhaust time in terms of the duct opening size and discharge coefficient.

The flexibility needed for in-flight evaluation of the proposed method was achieved by constructing the exhaust duct like a conventional duct (see Figures 1 and 4). Once a proper value of S_D was determined, the duct could be tied shut at that level with a squibbed line and the lower portion trimmed off. At the proper time, the squib could be fired by command and the exhaust duct would open. Selection of this approach to achieving the desired vertical location made it possible to buy balloons without one having exact knowledge of the required negative lift.

When this approach was first attempted there was an alternate explanation of the relationship between the exhaust duct's location and the volume to be exhausted. It suggested that the exhausting process would proceed until the pressure across the

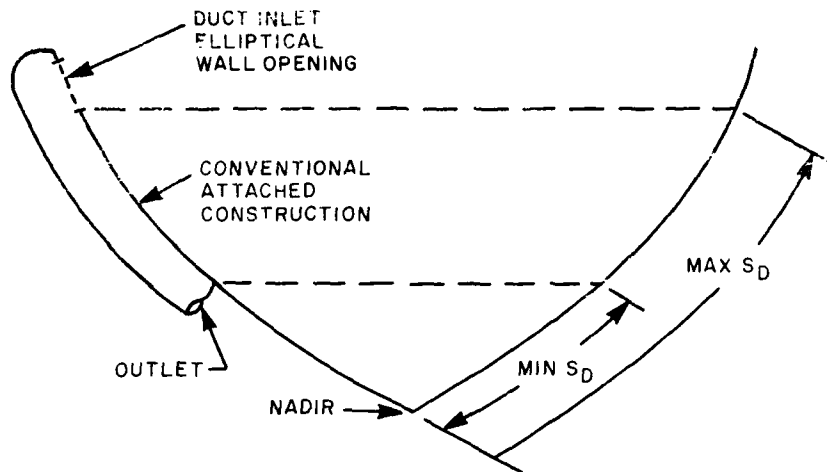


Figure 4. Pictorial Representation of the Flexibility Provided by Construction of the Exhaust Duct as a Conventional Ascent Valving Duct

mouth of the duct was equal to ambient pressure, at which point the shape and volume would conform to the family of classical subpressure shapes,⁴ and that the relationship of S_D to final volume would be characterized according to Figure 5. In accordance with this explanation, S_D for the first two trial applications* was chosen to be 40 ft to create a negative lift of about 5.5 percent (189 lb). However, according to the former theory, the resulting negative lift would have been about 10 percent of this value (about 18 lb). In neither of the flights was there any perceptible descent when the duct was opened.

A second experimental verification of the exhausting process was to be made using balloons, 12.44 million cu ft in volume, floating in the vicinity of 160,000 ft. Two flights, H71-35 and H71-36, were planned as simultaneous launches, but H71-35 was aborted on the ground before launch. On flight H71-36, the radar data located the balloon initially above 160,000 ft, and in the vicinity of 138,000 ft at duct activation and flight termination. At 138,000 ft, the balloon had a classical subpressure shape and the volume was only 40 percent of the volume at 160,000 ft. The value of S_D for the exhaust duct on this balloon type was 189 ft. At termination the zero pressure differential location was about 15 ft further up the gore. This

4. Smalley, J.H. (1964) Determination of the Shape of a Free Balloon, AFRL-65-72, Scientific Report No. 3, Contract No. AF19(628)-2783, AD 611 325.

*The first use of such a system was on flight H79-58 on 13 October 1970, and the second on flight H71-16 on 4 April 1971. In both cases the balloon had a volume of 5,136,000 cu ft and the float altitudes were about 105,000 ft.

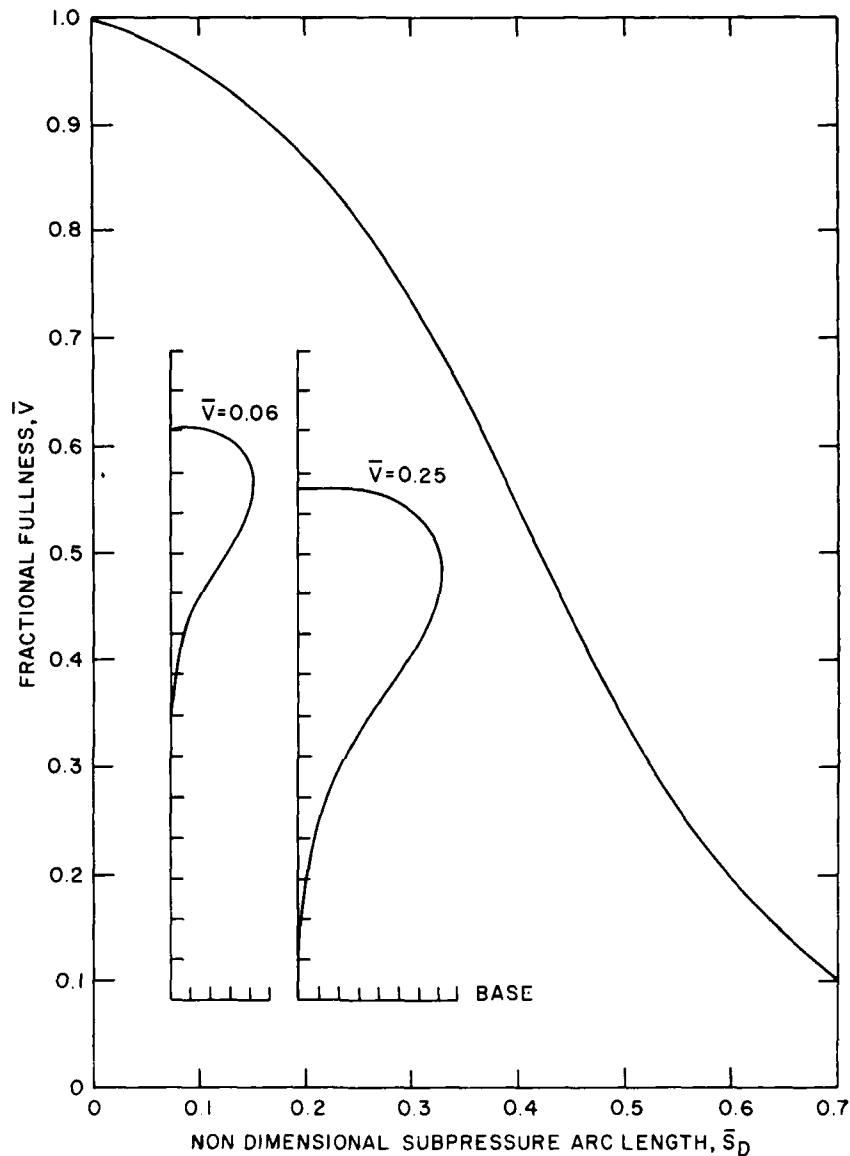


Figure 5. Volume Expressed as a Fraction of Maximum Balloon Volume in Relation to the Nondimensionalized Gore Length Distance, \bar{S}_D , from the Nadir to the Exhaust Duct Outlet or Zero Pressure Differential Level. The curve was developed from weightless cylinder balloon data⁵ and subsequently confirmed by actual balloon flights. The value of \bar{S}_D has been nondimensionalized with respect to the balloon gore length. The inserts show subpressure balloon shapes for differing values of fractional fullness

5. (1953) Progress Report on High Altitude Plastic Balloons, Volume V, Univ. of Minnesota, Contract No. NONR-710(01), Section III-B.

being the case, the pressure differential at the outlet of the exhaust duct caused intake of air rather than exhausting of helium.

The inconclusive results of these early "piggy-back" experiments, attributed to poor duct location on the first two flights and to the subpressure shape configuration at test time on the third flight, prompted the formal study, Work Unit 76591102.

5. THE SOPHISTICATED APPROACH

Among other things, the simple approach ignored balloon shape change, system descent and its aerodynamic characteristics, and the thermodynamic effects on buoyancy. Further, it seriously underestimated the potential consequences of subpressurization.

The significance of the subpressure shape, made evident by the performance of flight H71-36, was considered to be an aspect of the problem that should and could be addressed in a new study. Earlier experience in deflating a balloon during a hangar test seemed most pertinent. At that time, a large hole in the base of the balloon was used to significantly increase the rate of gas flow through the apex valve (much like the second hole punched in a juice can allows air to flow in and thereby avoids the tendency toward a vacuum). This approach was considered both adequate and practical as a means of avoiding sub-pressurization and its undesired effects.

An axially concentric inlet duct at the nadir (see Figure 6), by enabling air to flow in below the lifting gas, would prevent formation of a subpressure shape. However, the attendant shape changes would require a new model to approximate the new shapes. The so called parachute shape,^{*} an obvious choice, was too complex and time consuming to be computationally practical. A compromise model was chosen and is described in Appendix B.

The compromise model is comprised of a "natural shape" and an inverted cone, co-axial with it and tangentially appended to it. The inflation gas is assumed to occupy the volume above the plane of tangency, and the ingested air is assumed to occupy the conical volume below the aforementioned plane. Since the arc length between apex and nadir in the plane containing the vertical axis is the constant

*The parachute shape is that shape resulting from inclusion of air (at ambient conditions) below the base level of the inflatable. Otherwise the shape is governed by the Smalley codes.⁶ This shape was used by the author to analyze the failure of a CRISP program balloon.

6. Smalley, J. H. (1965) Determination of the Shape of a Free Balloon (Summary), AFRL-65-92, Final Report, Contract No. AF19(628)-2783, AD 614 610.

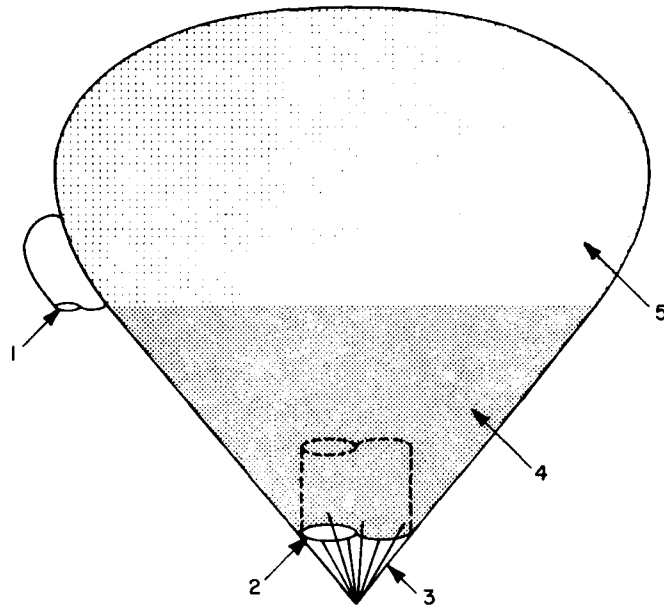


Figure 6. Simplified Parachute Shape Model. The components are: 1) exhaust duct, 2) inlet duct, 3) load tapes, 4) ingested air, and 5) lifting gas

balloon gore length, the ratio of the instantaneous volume of inflation gas to the fixed theoretical maximum volume uniquely determines the cone angle at the nadir and all other balloon shape dimensions. This model is preferable to one similarly defined using a spherical shape, if only because of the improved accuracy of dimensions when the balloon is nearly full—the condition predominating in this problem.

Consideration of shape changes due to the venting of inflatant and the ingestion of air, made it desirable and reasonable to account also for shape and volume changes due to re-compression of the confined gases during descent. This was accomplished using three differential equations to describe the system changes with respect to time: velocity change, altitude change and volume change. Pertinent atmospheric properties were modeled in accordance with a single equation, I. 2. 10-(3), part of the model for the U. S. Standard Atmosphere.⁷ Use of the value, $10^{-5} \text{ } ^\circ\text{C}/\text{km}$ (geopotential), for the gradient of the molecular scale temperature wherever that gradient was identically equal to zero made it possible to reduce the model to a single function.

7. (1962) U. S. Standard Atmosphere, 1962, published by U. S. Committee on Extension to the Standard Atmosphere; USAF, NASA, USWB.

The shape model and exhaust system were analyzed in computer simulated flights. The ratio of cone volume (see Eq. (7)) to maximum balloon volume was found to be the maximum possible fractional heaviness (as opposed to fractional free lift). Faster shape changes with increased descent rates caused the achieved fractional heaviness to decrease, a favorable relationship limiting the lift loss. Tables 1 and 2 contain simulated model responses for assumed drag coefficients of 0.5 and 1.0 respectively.

In order to evaluate the exhausting process and the system responses thereto (including feedback effects) the balloon described in Table 3 was designed and two units were fabricated for flight testing in the Summer of 1979. Plans for the two test flights (H79-32, 27 June and H79-34, 15 July) were essentially identical. The exhaust ducts on these balloons were located to enable a maximum fractional heaviness of 0.044 using the upper duct and 0.027 using the lower duct.

Tables 4 and 5 show the reactions of flights H79-32 and H79-34 in response to activation of the exhaust systems. For the former flight, the upper exhaust duct was opened and for the latter, the lower one.

The results of Flight H79-32 were dramatic, although disappointing. Never, except in the case of balloon malfunction, have such descent rates been so rapidly achievable during the morning when the inflatant is subject to solar heating. The approximate average descent rates in feet per minute (at about 2-min intervals) over the first twelve minutes were: 870, 580, 475, 390, 315 and 290. Clearly a significant volume of gas was lost rapidly, and clearly either the flow was stanching or the magnitude of the thermodynamic effects was underestimated. The answer was to be found in the analysis of the motion picture films of the exhaust sequence.

Flight H79-34 did not exhibit the type of response observed on its twin. Its nondescript reactions were barely distinguishable from normal short-term altitude variations.

The performances of flights H79-32 and H79-34 were clarified by the up-camera films. In neither flight did the base inlet duct perform as it was designed to do. Although the post-flight inspection of the balloon revealed that the line cutters performed properly, the ducts did not open. These failures were attributed to entrapment of the respective ducts by the closely spaced, highly tensioned load tapes. In both flights the base of the duct protruded through the web of tapes at launch and apparently stayed so throughout the flight.

On flight H79-32 the balloon must have lost lift; this was evidenced not only by the initial descent response but also by the up-camera film. Not so surprisingly (in retrospect), the ascent valving ducts fully collapsed, as did the exhaust duct, both indicating that the level of zero pressure differential had moved upward to a point above the exhaust duct outlet, stanching the flow of gas. Some implications of this are discussed in the conclusions of this report.

Table 1. Balloon Performance With a Drag Coefficient of 0.5. These are the results of computer-simulated system response of a modified parachute-shape balloon, 2.37 million cu ft in volume with an exhaust duct 30 sq ft in area, with its outlet approximately 70 ft up the gore from the balloon nadir. The minus sign indicates force or motion downward toward the earth

Time (min)	Head (ft)	Force (pct)	Alt. (ft)	Vel. (fpm)
0.00000E+00	4.13125E+01	0.00000E+00	1.00000E+05	0.00000E+00
5.00000E-02	3.02971E+01	-1.76097E-01	9.99999E+04	-4.50718E+00
1.00000E-01	2.78081E+01	-3.40345E-01	9.99994E+04	-1.73886E+01
1.50000E-01	2.63085E+01	-4.98816E-01	9.99981E+04	-3.81974E+01
2.00000E-01	2.49162E+01	-6.53326E-01	9.99955E+04	-6.65195E+01
2.50000E-01	2.35983E+01	-8.04040E-01	9.99913E+04	-1.01836E+02
3.00000E-01	2.26668E+01	-9.52174E-01	9.99852E+04	-1.43506E+02
3.50000E-01	2.17296E+01	-1.09868E+00	9.99768E+04	-1.90780E+02
4.00000E-01	2.07841E+01	-1.24416E+00	9.99660E+04	-2.42780E+02
4.50000E-01	1.98301E+01	-1.38930E+00	9.99525E+04	-2.98521E+02
5.00000E-01	1.88705E+01	-1.53491E+00	9.99361E+04	-3.56970E+02
5.50000E-01	1.79110E+01	-1.68180E+00	9.99168E+04	-4.17093E+02
6.00000E-01	1.69601E+01	-1.83081E+00	9.98944E+04	-4.79919E+02
6.50000E-01	1.60297E+01	-1.98271E+00	9.98690E+04	-5.38581E+02
7.00000E-01	1.51339E+01	-2.13821E+00	9.98406E+04	-5.98358E+02
7.50000E-01	1.42893E+01	-2.29792E+00	9.98092E+04	-6.56690E+02
8.00000E-01	1.35139E+01	-2.46238E+00	9.97749E+04	-7.13182E+02
8.50000E-01	1.26043E+01	-2.63194E+00	9.97379E+04	-7.67594E+02
9.00000E-01	1.17494E+01	-2.80626E+00	9.96982E+04	-8.19800E+02
9.50000E-01	1.09094E+01	-2.98569E+00	9.96559E+04	-8.69782E+02
1.00000E+00	1.00822E+01	-3.17029E+00	9.96113E+04	-9.17612E+02
1.05000E+00	9.26621E+00	-3.36008E+00	9.95642E+04	-9.63419E+02
1.10000E+00	8.46036E+00	-3.55505E+00	9.95149E+04	-1.00737E+03
1.15000E+00	7.66361E+00	-3.75518E+00	9.94635E+04	-1.04964E+03
1.20000E+00	6.87514E+00	-3.96046E+00	9.94100E+04	-1.09042E+03
1.25000E+00	6.09421E+00	-4.17087E+00	9.93545E+04	-1.12991E+03
1.30000E+00	5.32015E+00	-4.38639E+00	9.92970E+04	-1.16826E+03
1.35000E+00	4.55233E+00	-4.60705E+00	9.92377E+04	-1.20563E+03
1.40000E+00	3.79019E+00	-4.83284E+00	9.91765E+04	-1.24218E+03
1.45000E+00	3.03316E+00	-5.06379E+00	9.91135E+04	-1.27801E+03
1.50000E+00	2.28076E+00	-5.29994E+00	9.90487E+04	-1.31324E+03
1.55000E+00	1.53250E+00	-5.54132E+00	9.89822E+04	-1.34796E+03
1.60000E+00	7.87955E-01	-5.78799E+00	9.89139E+04	-1.38225E+03
1.65000E+00	0.00000E+00	-6.04002E+00	9.88439E+04	-1.41618E+03

Table 2. Balloon Performance With a Drag Coefficient of 1.0. These are the results of computer-simulated system response of a modified parachute-shape balloon, 2.37 million cu ft in volume with an exhaust duct 30 sq ft in area, with its outlet approximately 70 ft up the gore from the balloon nadir. The minus sign indicates force or motion downward toward the earth

Time (min)	Head (ft)	Force (pct)	Alt. (ft)	Vel. (fpm)
0.00000E+00	4.13125E+01	0.00000E+00	1.00000E+05	0.00000E+00
5.00000E-02	3.02971E+01	-1.76097E-01	9.99999E+04	-4.50663E+00
1.00000E-01	2.78081E+01	-3.40345E-01	9.99994E+04	-1.73724E+01
1.50000E-01	2.63087E+01	-4.98816E-01	9.99981E+04	-3.80813E+01
2.00000E-01	2.49168E+01	-6.53324E-01	9.99955E+04	-6.60535E+01
2.50000E-01	2.35998E+01	-8.04027E-01	9.99913E+04	-1.00485E+02
3.00000E-01	2.26711E+01	-9.52116E-01	9.99853E+04	-1.40335E+02
3.50000E-01	2.17397E+01	-1.09849E+00	9.99772E+04	-1.84377E+02
4.00000E-01	2.08048E+01	-1.24363E+00	9.99669E+04	-2.31237E+02
4.50000E-01	1.98686E+01	-1.38806E+00	9.99541E+04	-2.79506E+02
5.00000E-01	1.89356E+01	-1.53229E+00	9.99389E+04	-3.27866E+02
5.50000E-01	1.80131E+01	-1.67681E+00	9.99213E+04	-3.75192E+02
6.00000E-01	1.71099E+01	-1.82201E+00	9.99014E+04	-4.20627E+02
6.50000E-01	1.62362E+01	-1.96823E+00	9.98793E+04	-4.63604E+02
7.00000E-01	1.54028E+01	-2.11572E+00	9.98551E+04	-5.03826E+02
7.50000E-01	1.46207E+01	-2.26469E+00	9.98290E+04	-5.41225E+02
8.00000E-01	1.39005E+01	-2.41532E+00	9.98010E+04	-5.75900E+02
8.50000E-01	1.32521E+01	-2.56776E+00	9.97714E+04	-6.08061E+02
9.00000E-01	1.24091E+01	-2.72167E+00	9.97403E+04	-6.37982E+02
9.50000E-01	1.16847E+01	-2.87704E+00	9.97077E+04	-6.65935E+02
1.00000E+00	1.09805E+01	-3.03391E+00	9.96737E+04	-6.92194E+02
1.05000E+00	1.02942E+01	-3.19227E+00	9.96385E+04	-7.17013E+02
1.10000E+00	9.62367E+00	-3.35213E+00	9.96020E+04	-7.40616E+02
1.15000E+00	8.96732E+00	-3.51348E+00	9.95644E+04	-7.63195E+02
1.20000E+00	8.32370E+00	-3.67632E+00	9.95257E+04	-7.84912E+02
1.25000E+00	7.69153E+00	-3.84068E+00	9.94859E+04	-8.05900E+02
1.30000E+00	7.06974E+00	-4.00657E+00	9.94451E+04	-8.26269E+02
1.35000E+00	6.45736E+00	-4.17402E+00	9.94033E+04	-8.46108E+02
1.40000E+00	5.85354E+00	-4.34305E+00	9.93605E+04	-8.65488E+02
1.45000E+00	5.25753E+00	-4.51369E+00	9.93168E+04	-8.84469E+02
1.50000E+00	4.66864E+00	-4.68597E+00	9.92721E+04	-9.03100E+02
1.55000E+00	4.08629E+00	-4.85993E+00	9.92265E+04	-9.21420E+02
1.60000E+00	3.50993E+00	-5.03561E+00	9.91799E+04	-9.39463E+02
1.65000E+00	2.93908E+00	-5.21302E+00	9.91325E+04	-9.57257E+02
1.70000E+00	2.37330E+00	-5.39222E+00	9.90842E+04	-9.74825E+02
1.75000E+00	1.81219E+00	-5.57324E+00	9.90350E+04	-9.92190E+02
1.80000E+00	1.25539E+00	-5.75611E+00	9.89850E+04	-1.00937E+03
1.85000E+00	7.02589E-01	-5.94086E+00	9.89341E+04	-1.02638E+03
1.90000E+00	1.53475E-01	-6.12754E+00	9.88824E+04	-1.04323E+03
1.91250E+00	0.00000E+00	-6.17448E+00	9.88693E+04	-1.04743E+03

Table 3. Characteristics of Flight Test Balloon, AFGI Model No. LTV-026, Equipped With Stub Exhaust Ducts

Characteristics	Value	Units
Volume	2,370,000	cu ft
Gore length	260	ft
Σ	0.15	-
Film thickness	0.0015	in
Number of gores	67	-
Number of ducts (valving)	2	-
Duct area (valving)	25	sq ft
Number of exhaust ducts	2	-
Exhaust duct area	30	sq ft
Upper exhaust duct	70.5	ft
Lower exhaust duct	67.5	ft

Table 4. Time-Altitude System Response of Flight H79-32

Time (local)	Altitude (ft)	Time (local)	Altitude (ft)
8:46: 8	98932	8:53:13	95887
8:46:25	98759	8:53:30	95887
8:46:42	98371	8:53:47	95916
8:46:59	98170	8:54: 4	95815
8:47:16	97854	8:54:21	95873
8:47:33	97639	8:54:38	95772
8:47:50	97380	8:54:55	95858
8:48: 7	97194	8:55:12	95873
8:48:24	96935	8:55:29	95873
8:48:41	96792	8:55:46	95901
8:48:58	96605	8:56: 3	95786
8:49:15	96634	8:56:20	95729
9:49:32	96634	8:56:37	95729
8:49:49	96634	8:56:54	95643
8:50: 6	96605	8:57:11	95514
8:50:23	96533	8:57:28	95528
8:50:40	96461	8:57:45	95485
8:50:57	96303	8:58: 2	95470
8:51:14	96303	8:58:19	95456
8:51:31	96160	8:58:36	95514
8:51:48	96131	8:58:53	95470
8:52: 5	96074	8:59:10	95470
8:52:22	96002	8:59:27	95499
8:52:39	96002	8:59:44	95456
8:52:56	95901	9: 0: 1	95499

Table 5. Time-Altitude System Response of Flight H79-34.
 The asterisk at the time entry 9:09:00 indicates the time
 when the second duct was opened

Time (local)	Altitude (ft)	Time (local)	Altitude (ft)
8:58:41	98888	9:13:15	96576
8:58:58	98917	9:13:32	96490
8:59:15	98903	9:13:49	96476
8:59:32	98874	9:14: 6	96447
8:59:49	98874	9:14:23	96490
9: 0: 6	98616	9:14:40	96461
9: 0:23	98486	9:14:57	96375
9: 0:57	98099	9:15:14	96404
9: 1:14	97998	9:15:31	96375
9: 1:31	97926	9:15:48	96390
9: 2: 5	97610	9:16: 5	96404
9: 2:23	97582	9:16:22	96361
9: 2:58	96964	9:16:39	96375
9: 3:48	97452	9:16:56	96390
9: 6: 3	97251	9:17:13	96332
9: 6:20	97151	9:17:30	96332
9: 7: 0	97050	9:17:47	96390
9: 7:18	97050	9:18: 4	96375
9: 7:35	97079	9:18:21	96318
9: 7:52	96978	9:18:55	96318
9: 8: 9	96993	9:19:12	96318
9: 8:26	96978	9:19:29	96246
9: 8:43	96964	9:19:46	96131
9: 9: 0*	96935	9:20: 3	96088
9: 9:17	96950	9:20:20	96031
9: 9:34	96907	9:20:37	96002
9: 9:51	96892	9:20:54	96031
9:10: 8	96806	9:21:11	96002
9:10:25	96749	9:21:28	96059
9:10:42	96662	9:21:45	96031
9:10:59	96677	9:22: 2	96045
9:11:16	96634	9:22:19	96016
9:11:33	96591	9:22:36	96016
9:11:50	96605	9:22:53	96074
9:12: 7	96591	9:23:10	96016
9:12:24	96619	9:23:27	96002
9:12:41	96447	9:23:44	96031
9:12:58	96548	9:24: 1	95786

To eliminate its entrapment on the next series of balloons designed to test the descent method, the inlet duct, after being equipped with its squib-operated line cutter, was inverted upward for its entire length into the balloon envelope. In this manner, the duct would be held during ascent, first by the undeployed film and then by the subpressure, until the conical cage of load tapes radiating from the base end-fitting was positioned and fully tensioned. The duct, it was hoped, could not then be pinched off or held by the cage of rigid tapes.

In addition to the aforementioned change, both the height and construction of the exhaust ducts were changed. The lower exhaust duct was constructed as a "horse tail" type (see Figure 3) with its envelope wall opening centered 67.5 ft up the gore from the base end fitting. The upper exhaust duct was constructed as a standard attached duct, entering the envelope 100.7 ft up from the base end fitting. Where the outlet of the lower duct was fixed at a height 6 ft below its envelope entry point, the outlet of the upper duct could be set just before balloon inflation at any distance between 66.5 ft and 90.5 ft, measured along the gore from the base end fitting. (See Figure 4.)

The first of two redesigned balloons was launched as flight number H80-05 at 1401Z on 2 February 1980. The upper duct, with its outlet located 77 feet up from the base end fitting, was activated at 1609:30Z; 6 minutes later the balloon started its descent from 98,662 ft. After an irregular descent for 10 minutes, the system started to float at 95,352 ft. For practical purposes, the experiment had failed.

The up-camera film confirmed the suspicion that the base inlet duct had once again failed to open. At that time it was decided to eliminate the engineering problem—inlet duct design to prevent entrapment. The flight preparation plan for unit number two was thus amended to include removal of the inlet duct, thereby creating an open base balloon.* The modification was effected with no difficulty, and the balloon was launched as flight H80-07 on 5 February 1980 at 1344Z. As the balloon ascended and filled out, its nadir cone angle increased to the extent that the opening in the base became a free passage between the balloon interior and the atmosphere. At that time air ingestion resulting from subpressurization began to influence the ascent rate. Ascent rate data, in feet per minute, taken over successive intervals (20-min) between 45,000 ft and float altitude were, 780, 700, 600, 360 and 195, behavior not common to conventional closed-base balloons.

At 1702Z, with the balloon system floating at 99,366 ft, the experiment was initiated. It was more than 6 minutes before any trend was discernible, even though the second (lower) exhaust duct had been opened at 1705Z. At 1725Z the system entered a 5-min float at 94,919 ft and subsequently dropped to 94,516 ft at 1732:30Z where it remained for about 4.5 min. At that time the performance

*The open base balloon, unusual today, was commonplace in the early 1950's before the invention of the ascent valving duct.

suggested that the thermodynamics of the ingested air was probably the dominating factor, and that the purpose of the descent system could not be accomplished.

According to a contingency plan, the apex valve was latched open at 1737Z to gather data on system response to valving under the uniquely different situation provided by an open-base balloon. The valve was held open for 23 min, during which time the system descended slightly more than 4,600 ft. The descent rate at the time of termination, 1806Z, was little more than the 200 ft per min experienced during the valving exercise.

The final useful information was provided by vertically oriented flight cameras. The relative contrast in the appearance of the open base on this flight left no doubt that the inlet ducts on the previous flights were in fact closed. Although the outlet ends of the exhaust ducts were not visible due to sunlight reflecting from the balloon, the overpressure relief ducts were quite distinct. Full when the experiment was started, the relief ducts gradually collapsed as the zero pressure differential plane moved from the plane of the base opening to the plane of the outlets of the exhaust ducts. From a mechanical standpoint, the modified system worked as designed.

6. CONCLUSIONS

The indisputable result of this study is that there still exists no technique to initiate balloon system descent from high altitudes: descent at rates that are predictable, controllable and, within physical limitations, instantaneously achievable.

It is essential to remember that the loss of lifting gas is not, in itself, sufficient to effect descent. The necessary and sufficient condition is that the weight of air displaced by the system be less than the gross weight of the system. Thus, the requirement that the desired descent rate be, for practical purposes, instantaneously achievable means that either the gross weight of the system or the "effective volume" of the balloon be instantaneously alterable.

The results of flight H80-7 indicate that the "effective volume" was not dramatically or significantly altered. If the air ingested into the base cone had followed the ambient temperature, the "effective volume" of the balloon would have been reduced by the volume of the cone and the buoyant force would have been diminished proportionately. The performance indicated that the ingested air remained at or above the integrated average temperature of its original level(s) as the balloon "sank" into a colder, denser environment. This behavior was no doubt influenced by the warming of the air as it compressed during the descent.

Flight H80-7 proved that it is not practical to use air ingestion to effect a free lifting gas surface at the nadir and thereby to achieve a desired discharge velocity which is proportional to the square root of the velocity head.

7. THE NEXT STEPS

An "effective free surface" at the nadir is theoretically attainable by having the conical surface detached from the load tapes for the length of its slant height. This would allow the cone envelope material to (so to speak) "float" upward as the gas flows out. Thereby the balloon's shape and volume would be changed, and the formation of a subpressure region would be avoided. However, when the system passed below the altitude at which the cone would be exhausted, the envelope would be drawn upward by the recompression of the remaining lifting gas, and would be blown upward and inward by descent ram air pressure. The resulting forces would probably be sufficient to cause the balloon envelope to rupture at its juncture with the detached conical surface.

If we assume (but not necessarily concede) that achievement of a "free surface" at the nadir is not practical, we face the problem that an unforced exhausting process must work against a developing subpressure region. The initial response of the balloon system on flight H79-32 supplied evidence of the kind of response that might be expected with such a system.

When evaluated in conjunction with the motion picture film, which showed the upward progress of the level of zero pressure differential, the resultant descent rates for flight H79-32 force the conclusion that some air was ingested. Specifically, the final position of the level of zero pressure differential assures that the final relative location of the outlet of the exhaust duct was in the sub-pressure region. Although the film provided no proof that air was ingested, it likewise provided no proof that air was not ingested. Finally, the drop off of the descent rate is consistent with the behavior of such a system after having ingested air.

The principal unanswered question with respect to performance of the latter type of system is then: what is the relationship between the volume of inflatant exhausted and the length of arc between the nadir and the location of the zero differential pressure level? The performance of flight H79-32 suggests that the relationship shown in Figure 5 is not unique and that there are other equally valid relationships between the dimensionless arc length, \bar{S}_D , and the fractional fullness. Were this not so, the zero pressure differential level could not have moved as high as it did. The non-uniqueness of the relationship is further suggested by the performance of some balloons that, when rising rapidly, failed to level off at altitudes consistent with their altered duct lengths; the actual performances were, however, consistent with a relationship permitting at least two values of fractional fullness for a single value of \bar{S}_D .

Successful development of a quick descent system, independent of the need both to clarify the aforementioned relationship and to conduct validation test flights, would of course rest upon the ability to prevent air ingestion with its attendant

adverse thermodynamic effects. Further, since it is the location of the exhaust duct outlet that controls the lift loss rate and amount, there are advantages to be gained by having the duct's opening mechanism (assumed to be a line and line cutter) located at or near the balloon wall opening (the duct inlet). One advantage is that the installation can be made during the balloon manufacturing process rather than during balloon launch preparation: thereby the possibility of damage to the balloon is reduced. A second advantage is that the ability to adjust a duct's outlet location is not compromised by this design. It is, therefore, recommended that this design feature be used for similar balloon duct applications in the future.

A pertinent fact evidenced by these flights (except H80-07) is that the ducts collapsed, meaning that the lifting gas that had been in them was exhausted back through the balloon as it must also be when using an apex valve. This phenomenon with respect to valving has not been reported in the literature and has implications with respect to normal apex valving as well as to the quick descent problem.

8. SUPPLEMENTARY RESULTS

Two additional bits of information are worth documenting. One was the result of an accident and the other was obtained as a by-product related to the balloon shape selected for the flight test units.

In 1972, due to repeated problems with entanglement of the internal apex portion of the balloon destruct line system, the author designed a webbed variation based on the principle that webs and ribbons have a natural antisnagging tendency not common to lines, cables, or strings. The system was proved to be reliable and is now used routinely on Air Force balloons. Such a webbed system was installed improperly in the balloon used on flight H80-05.

The mislocation of the destruct buttons on the balloon used for flight H80-05 caused the rip panels to be severely loaded during inflation. Subsequently, when the balloon was released from the launch platform, the buttons were dynamically loaded to the extent that one button was ripped from the balloon wall, leaving a hole, approximately 4 sq in in area and 20 ft radially outward from the apex fitting. Surprisingly, the hole did not propagate and did not discernibly affect flight performance. An extremely porous piece of kimpak, used to cover the button, did remain over the hole and, evidently, limited the gas loss.

Perhaps the most interesting finding resulted from the intentional use of a balloon shape designed to accommodate payloads heavier than those flown on flights, H79-32, H79-34, H80-05, and H80-07. As a consequence, the balloons (in flight) tended toward higher than design degrees of oblateness, characterized by full deployment of the circumferential material. This fullness manifested itself in flight

performance to the extent that the amplitudes of the normal sine wave oscillations (following float entry) were noticeably lower than usual, according to the flight meteorologist.

It is theorized that a significant contributor to the normally observed oscillation amplitude is the "potential volume" made possible by excess circumferential material. It has been the practice, since the development of the natural shape,⁸ to design the balloon shape for the minimum payload and to design the balloon load structure for the maximum payload. This practice was initiated to "theoretically" guarantee⁹ that the circumferential stress would be zero over the entire design payload range. Consequences of this are excess circumferential material and deficient volume at any payload greater than the design minimum.*

Such oscillations have been a continuing concern to those studying the vertical motions of zero pressure balloons (see References 10 and 11 for early examples). It is believed that a proper balloon shape (as in this study) will eliminate volumetric changes that tend to mask thermodynamic and aerodynamic influences on vertical motions at "float" altitude.

*"Excess circumferential material" means envelope material, at all levels, in excess of the local balloon circumference. "Deficient volume" means that the achievable full volume is less than the fabricated maximum balloon volume.

8. Dayer, J.F. (1979) Zero pressure balloon shapes, past, present and future, in Proceedings, Symposium on the Scientific Use of Balloons (COSPAR 1978).
9. Bleich, H.H. (1963) An Investigation of High-Altitude Balloons of Shapes Which Are Not Rotationally Symmetric, Columbia University, Final Report, Contract No. Nonr 266(87).
10. Nishibara, J. and Hirose, H. (1969) On the hunting mechanism of the plastic balloon, in Proceedings of the Eighth International Symposium on Space Technology and Science, Tokyo, Japan, pp. 1157-1161.
11. (1953) Progress Report on High Altitude Plastic Balloons, Volume V, Univ. of Minnesota, Contract No. NC NR-710(01), Section VI.

References

1. Dwyer, J. F. (1974) Free balloon capabilities: a critical perspective, in Proceedings (Supplement), Eight AFCRL Scientific Balloon Symposium, 30 September to 3 October 1974, AFCRL-TR-74-0596, ADA008 489. pp 123-156.
2. Schwoebel, R. L. (1956) Strato-lab Development, General Mills, Inc., Report No. 1648, Final Report, Contract No. NONR 1589(06).
3. Dwyer, J. F. (1973) Balloon Apex Pressure Differential, AFCRL-TR-73-0632, AD 774 399.
4. Smalley, J. H. (1964) Determination of the Shape of A Free Balloon, AFCRL-65-72, Scientific Report No. 3, Contract No. AF19(628)-2783, AD 611 825.
5. (1953) Progress Report on High Altitude Plastic Balloons, Volume V, Univ. of Minnesota, Contract No. NONR-710(01), Section III-B.
6. Smalley, J. H. (1965) Determination of the Shape of a Free Balloon (Summary), AFCRL-65-92, Final Report, Contract No. AF19(628)-2783, AD 614 610.
7. (1962) U. S. Standard Atmosphere, 1962, published by U. S. Committee on Extension to the Standard Atmosphere; USAF, NASA, USWB.
8. Dwyer, J. F. (1979) Zero pressure balloon shapes, past, present and future, in Proceedings, Symposium on the Scientific Use of Balloons (COSPAR 1978).
9. Bleich, H. H. (1963) An Investigation of High-Altitude Balloons of Shapes Which Are Not Rotationally Symmetric, Columbia University, Final Report, Contract No. Nonr 266(87).
10. Nishimura, J. and Hirose, H. (1969) On the hunting mechanism of the plastic balloon, in Proceedings of the Eighth International Symposium on Space Technology and Science, Tokyo, Japan, pp. 1157-1161.
11. (1953) Progress Report on High Altitude Plastic Balloons, Volume V, Univ. of Minnesota, Contract No. NONR-710(01), Section VI.

Appendix A

Notes on Flight C72-21

The record-setting performance of balloon flight C72-21, using a balloon 47.8 million cu ft in volume, was made possible by the development of a truly balloon-grade polyethylene film, 0.00035 in. thick. This development took place under Air Force contract number F19628-71-C-0042 with Winzen Research, Incorporated. Film suitability was determined under a subcontract performed by Dr. Harold Alexander and Mr. Dan Weissmann at an Air Force contract test laboratory at Stevens Institute of Technology, Hoboken, New Jersey.

The conclusion of the unpublished subcontract report on uniaxial and biaxial testing of the film is transcribed below.

"This 0.35 mil StratoFilm was found to be superior to all previous StratoFilms, except for its room temperature elongation and its creep strength at high temperatures. As a balloon film it will probably perform excellently at cold temperatures. Tropopause failures should not be a problem. It will, however be very sensitive to overloading at launch. A long hold, while inflated at high launch temperatures could be fatal to a balloon of this material. It is the opinion of the authors that, if that eventuality is prevented, a balloon fabricated of this material could be flown successfully, barring design and fabrication faults."

The significance of this development can be seen in the historical trends reported earlier^{A1} and here represented as Figure A1.

- A1. Dwyer, J. F. (1979) Required, a new zero pressure balloon shape, in Proceedings, Tenth AFGL Scientific Balloon Symposium, 21 August to 23 August 1978, AFGL-TR-79-0053, AD A074469, pp 165-170.

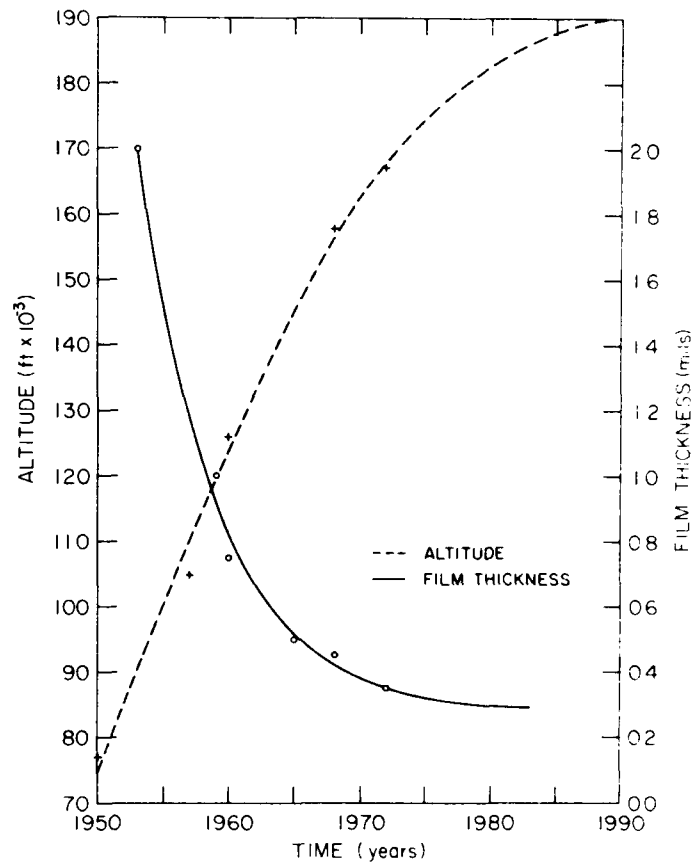


Figure A1. Historical Trends. These logistic curves best fit the data points and afford a degree of technology forecastability.

Appendix B

The Simplified Parachute-Shape Model

Figure B1 shows the essential features of the simplified parachute shape model created to approximate the shape of a balloon with ingested air in a layer below its inflation gas. There are two *principal invariants* that fix the shape. First, there is the assumed generator shape* with its nadir located at the origin of the indicated r-z coordinate system. Second, there is the co-axial cone of ingested air, tangent to the generator shape in the plane of the air-inflation gas interface.

Let σ and S be the gore lengths of the generator shape and full size model respectively. Further, let each be comprised of two complementary segments σ_1 and σ_2 and S_1 and S_2 respectively, the lower subscripted variables being the lengths below the air-inflation gas interface plane. Clearly σ_2 and S_2 are identical and S_1 is the slant height of the air-filled conical volume. Finally, let a bar over any geometrical dimension indicate non-dimensionalization with respect to σ^n , n being equal to 1 or 3 depending on whether the variable is a length or volume.

The air-inflation gas interface plane divides the generator shape volume, V_m , into an upper and a lower volume, V_2 and V_1 respectively, and establishes \bar{z} such that the variables \bar{r} , $\bar{\sigma}_1$, $\bar{\sigma}_2$, \bar{V}_1 , \bar{V}_2 , \bar{V}_m , and θ are uniquely determined. Theta, the cone angle, is the tangent angle in the plane of the generator shape axis of symmetry measured at the so-called interface plane.

*The generator shape used for the predictive portion of this study corresponded to an Upson natural shape ($\Sigma = 0.15$). This value was selected to correspond to the manufactured test balloon shapes.

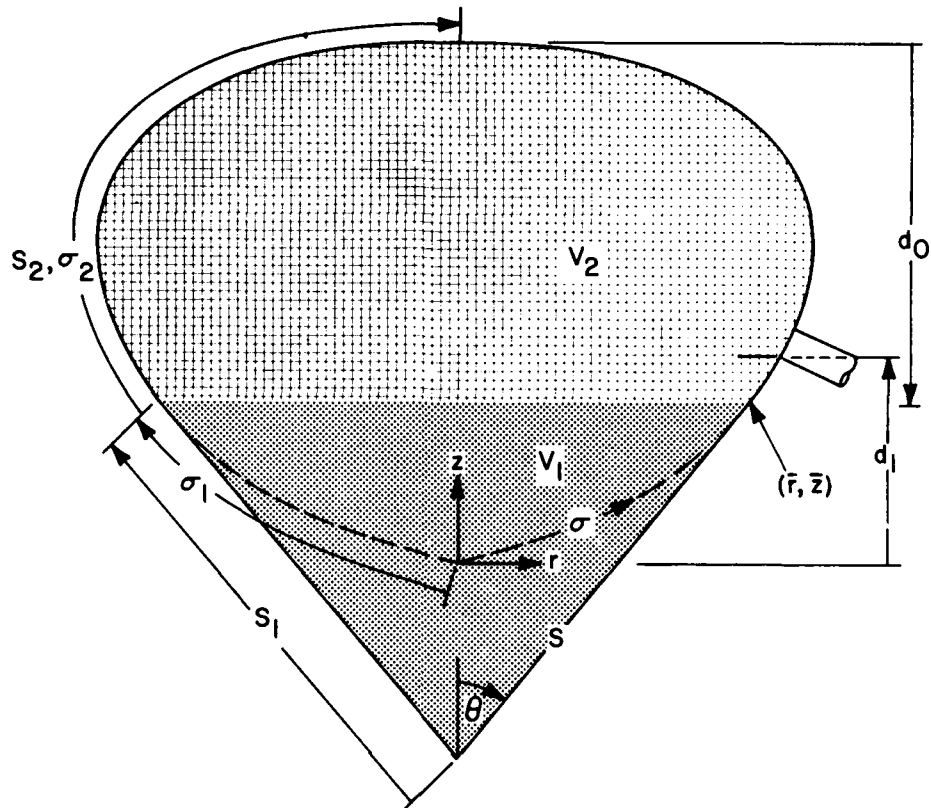


Figure B1. Essential Features of the Simplified Parachute Shape Model

From Figure B1 it is clear that:

$$\bar{S}_1 = \bar{r}/\sin \theta \quad (B1)$$

and, since $\bar{\sigma}_2$ and \bar{S}_2 are identical,

$$\bar{S} = \bar{\sigma}_2 + \bar{r}/\sin \theta \quad (B2)$$

yielding:

$$\sigma = S/(\bar{\sigma}_2 + \bar{r}/\sin \theta) \quad (B3)$$

Taking the cube of both sides of Eq. (B3) and multiplying by \bar{V}_2/V_{\max} (where V_{\max} is the maximum volume of the full size balloon), we obtain the fractional fullness (V_2/V_{\max}) as

$$(V_2/V_{\max}) = (1/\bar{V})(\bar{V}_2)/(\bar{\sigma}_2 + \bar{r}/\sin \theta)^3, \quad (\text{B4})$$

where:

$$\bar{V} = V_{\max}/S^3 = \text{constant for the specified } \Sigma.$$

Now, since \bar{z} has a maximum value, \bar{z}_{\max} , for the given generator shape, the depth of the inflation gas, d_o , is also uniquely determined by:

$$d_o = \sigma(\bar{z}'_{\max} - \bar{z}). \quad (\text{B5})$$

Finally, for a given S_o (the location of the exhaust duct with respect to its distance down the gore from the theoretical apex), the geometry of the constant generator shape allows one to use the non-dimensionalized position to solve for the vertical separation, d_1 , between the generator shape nadir and the horizontal plane of the exhaust duct. One can now solve for the head of gas, h , effecting the flow through the exhaust duct as

$$h = d_o - d. \quad (\text{B6})$$

Based on the unique relationship between \bar{r} and \bar{z} for the given generator shape and from the foregoing, it is seen that the model provides a unique relationship between the depth of the inflation gas and the fractional fullness of the balloon (independent of balloon size and shape), and further allows for the determination of the gas head.

The diameter and exposed surface area can likewise be determined for the consideration of aerodynamic and thermodynamic effects.

Mathematical representation of the model (Figure B2) relating \bar{z} to V_2/V_{\max} required the use of the eleven functions described in Table B1. The useful range of each function was selected to minimize the relative error in the computation of \bar{z} . In the computation process, the proper function is determined by comparison of the input value of V_2/V_{\max} with the sequentially smaller values of the lower limit of V_2/V_{\max} for each succeeding segment.

Table B2 lists the power series coefficients for computing θ (degrees), \bar{r} , and $\bar{\sigma}_1$ as functions of \bar{z} and for computing \bar{d}_1 as a function of $\bar{\sigma}_3$, where:

$$\bar{\sigma}_3 = \bar{\sigma} - (S - S_3)/\sigma \quad , \quad (B7)$$

and where σ_3 and S_3 are the distances between the nadir and the exhaust duct location on the generator shape and full-size model, respectively.

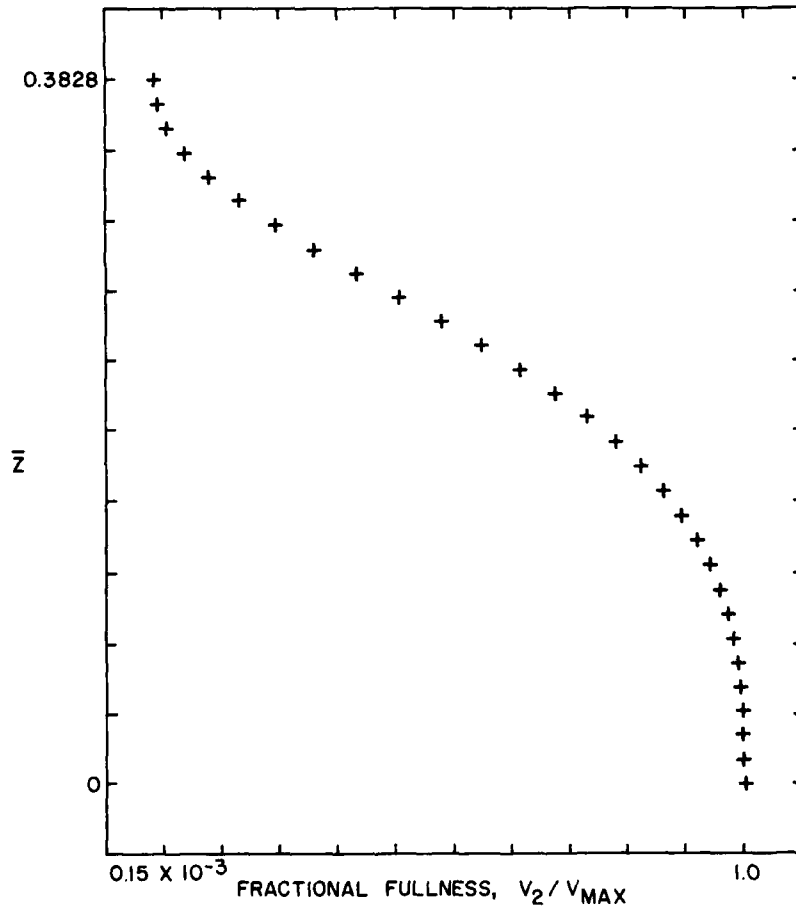


Figure B2. Plot of Data Points Used in the Functions that Model \bar{z} in Terms of V_2/V_{max}

Table B1. Functions Comprising Model to Solve for \bar{z} as a Function of V_2/V_{\max}

FUNCTION	QUADRATIC*	LINEAR	LINEAR
LIMIT	0.999685	0.998704865	0.996376
A0	1.00000000003E+00	1.34753263873E+01	5.70116144770E+00
A1	-5.33050188560E-03	-1.34631504373E+01	-5.66890344314E+00
A2	-2.46383176955E-01		
FUNCTION	LINEAR	POWER	QUADRATIC
LIMIT	0.99216	0.963	0.83035916
A0	3.17395699766E+00	1.57355741497E+01	9.24723778760E-01
A1	-3.13250803076E+00	-6.76591645350E+01	1.83075490637E+00
A2		9.06791946390E+01	-1.38588229434E+01
A3		-3.87067763930E+01	
FUNCTION	POWER	LINEAR	POWER
LIMIT	0.488	0.27218	0.0508769
A0	3.10918051082E-01	3.40858423189E-01	3.62984275675E-01
A1	2.77406825360E-01	-1.84925216085E-01	-4.37916794366E-01
A2	-2.63309861357E+00		1.02361964267E+00
A3	7.40613248360E+00		-1.44464774489E+00
A4	-1.10644856995E+01		
A5	8.48105265334E+00		
A6	-2.69143362928E+00		
FUNCTION	QUADRATIC	LINEAR	
LIMIT	0.00524869	0.00015	
A0	5.33921340740E+00	3.83179458027E-01	
A1	-2.81122836054E+01	-2.58720408811E+00	
A2	3.70145051127E+01		

*The coefficients A0, A1, and A2 correspond to the usual C, B, and A in the quadratic formula, and the sign of the radical is negative. The numerical index of the linear and power series coefficients corresponds to the exponent of the independent variable.

Table B2. Power Series Coefficients for Equations Defining Certain Relationships Between Elements of the Simplified Parachute Shape Model

Relationship	Coefficients	
$\theta = f(\bar{z})$	A0	56.151674
	A1	36.869415
	A2	-863.384153
	A3	4340.60078
	A4	-23751.1652
	A5	60663.6084
	A6	-55452.3401
$\bar{r} = f(\bar{z})$	A0	0.00012929
	A1	1.491118
	A2	0.89926756885
	A3	-12.4916446722
	A4	15.759250787
	A5	10.1738213142
	A6	-26.2026060888
$\bar{\sigma}_1 = f(\bar{z})$	A0	0.000128
	A1	1.791098667
	A2	0.901115015
	A3	-12.382923389
	A4	23.701897323
	A5	-8.8057025141
	A6	-8.2295252039
$\bar{d}_1 = f(\bar{\sigma}_3)$	A0	0.
	A1	0.550552495986
	A2	-0.011969020353
	A3	0.30392629417
	A4	0.20603025668
	A5	3.13781572
	A6	-4.61057125867

DATE
FILMED
—8